

Chapter 2

Seismic Hazard along the Himalayan Arc: A Review from Geological and Geodetic Studies

“ Speak to the earth, and it should teach thee.”

Job 11:8

This chapter presents a thorough literature survey of geological and geodetic studies on the seismic hazard analysis along Himalaya. The chapter also provides a comparison of geological and geodetic slip rates of the Himalayan megathrusts.

Contents

2.1	Introduction	30
2.2	Seismic hazard along the Himalayan arc: An overview	30
2.3	Seismic hazard along the northwest Himalaya	35
2.3.1	Geological studies along the northwest Himalaya	35
2.3.2	Geodetic studies along the northwest Himalaya	38
2.4	Seismic hazard along the central Himalaya	44
2.4.1	Geological studies along the central Himalaya	45
2.4.2	Geodetic studies along the central Himalaya	47
2.5	Seismic hazard along the northeast Himalaya	51
2.5.1	Geological studies along the northeast Himalaya	52
2.5.2	Geodetic studies along the northeast Himalaya	53
2.6	Comparison of geologic and geodetic rates along the Himalayan arc	56
2.7	Summary	60

2.1 Introduction

When the upper layer of the Earth's crust is stressed, it accumulates strain which can be of brittle or elastic type. This changed form of the crust is known as crustal deformation, which gets restored to its original form (elastic deformation) or it can take a new formation (brittle deformation) through the release of the accumulated strain in terms of seismic or aseismic activity [255]. There has been a considerable amount of studies to understand the crustal deformation due to past earthquakes and to monitor the future ones. Analysis of uplifted scarps, deep trenching, and fluvial terraces of rivers through carbon dating allows geologists to find fault displacements and age of historical earthquakes along with their return periods [255, 321]. Geological studies are often supplemented by the space-based techniques of geodesy that provide precise data on crustal deformation process [252]. Geodetic techniques evolved particularly for two practical purposes, namely the astronomical positioning and the land surveying. Further, the geodetic techniques are routinely used to monitor crustal movements and surface deformations. The 1892 Sumatra earthquake was the first event that was studied using the method of geodetic triangulation by the Dutch Geodetic Survey (DGS) [188]. Surface displacement of ~ 2 m along a geological fracture (later identified as a branched fault of the Great Sumatra Fault) due to the 1892 Sumatra earthquake was found by measuring the changed angles of the survey monuments [188]. A similar change in the monument angles and vertical motion was also found along the front of the Himalayan arc due to the 1897 Shillong earthquake and the 1905 Kangra earthquake [169, 201]. During the past decade, remarkable advancements in geodetic techniques increase the surge of interest among scientists to understand the kinematics and dynamics of crustal deformation and associated earthquake potential.

In this regard, the current chapter discusses some of the important contributions from previous studies towards a better understanding of the occurrence of historical earthquakes and fault kinematics along the Himalayan arc. The literature survey of geological and geodetic studies is carried out along the northwest, central, and the northeast Himalaya.

2.2 Seismic hazard along the Himalayan arc: An overview

The Himalayan arc is poised to generate a series of major to great earthquakes, catastrophic to densely populated countries of the southeast Asia astride the orogenic belt.

Geological, historical, and space-based geodetic techniques have been used to assess the seismic hazard in terms of earthquake potential, strain release and accumulation, slip rate estimation, out of sequence faulting, and convergence rate along various subsections of the Himalayan arc. More insights to the seismic process in terms of fault coupling and fault kinematics (e.g., dip angle, width, length, rake, strike, locking depth, and surface location) are also evident along the Himalayan arc [e.g., 30, 34, 88, 111, 113, 114, 116, 154, 159, 162, 163, 219, 277, 306, 323].

Bilham et al. (2001) [34] divided the whole Himalayan arc into 10 segments to derive potential magnitude and slip for future earthquakes (Fig. 1.1). They notified that the potential magnitude in all segments is too high to generate $M_w > 8.0$ events, except in the rupture zones of the twentieth-century earthquakes (i.e., 1905, 1934, and 1950 earthquake) [34]. With the occurrence of two recent large earthquakes, namely the 2005 Kashmir earthquake and the 2015 Gorkha earthquake, Bilham (2019) [30] recalculated the potential magnitude and slip for future earthquakes along 15 segments of the Himalayan arc using all available data from paleoseismic trenching, historical records of great earthquakes, and GPS measurements (Fig. 1.1). It is observed that the potential magnitude along the central seismic gap and the eastern Bhutan has reached up to $M_w = 8.5$ for the future event [30], whereas the maximum magnitude in the rupture areas of previous earthquakes (i.e., the events in 1905, 1934, 1950, and 2005) are about $M_w \sim 7.8$. In the rupture zone of the 2015 Gorkha earthquake, the long-term stored energy has been completely released, indicating a less possibility of any large earthquake in the near future (Fig. 1.1) [30].

Bilham and Ambraseys (2005) [31] evaluated average convergence rate of < 5 mm/yr from past earthquakes and ~ 18 mm/yr from GPS observations. The observed slip deficit of ~ 13 mm/yr is sufficient to generate $M_w \geq 8.5$ earthquakes along the Himalayan arc [31].

Stevens and Avouac (2015) [277] derived convergence rate of MHT using geodetic observations (Fig. 2.1). The slip rate of the décollement varies from 13.3 ± 1.7 mm/yr to 21.2 ± 2.0 mm/yr over a fully locked MFT to 100 ± 20 km in the north (Fig. 2.1) [277]. Further, Stevens and Avouac (2016) [276] estimated moment deficit rate and magnitude of the overdue large earthquake corresponding to the estimated total moment deficit over the past 1000 years along the Himalaya (Fig. 2.1). They estimated interseismic coupling ratio to identify a locked zone across and along the MHT, where future large earthquakes might occur, or an aseismic barrier that can arrest earthquake ruptures (Fig. 2.1) [276].

They observed that the locked barrier of frontal arc accumulates a moment deficit rate of $15.1 \pm 1.0 \times 10^{19}$ Nm/yr for the whole Himalaya, suggesting the possibility of a millinery $M_w=9.0$ earthquake in the near future [276].

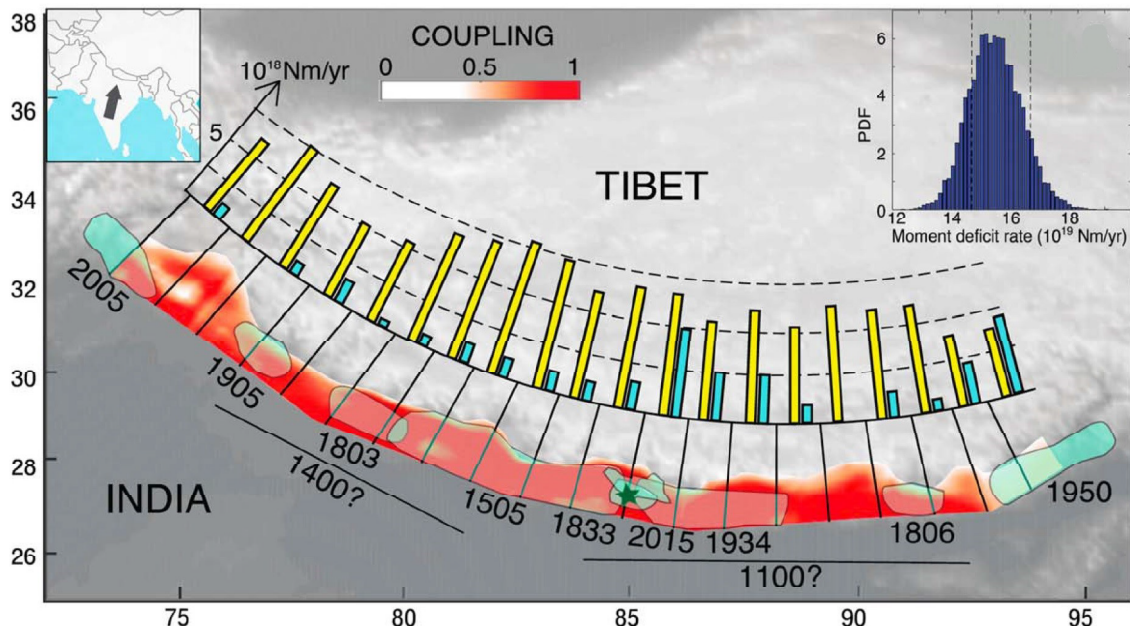


Fig. 2.1: The moment accumulation and fault coupling along the MHT. The red color indicates coupling pattern; the yellow bars show geodetic moment (posterior probability function for the geodetic moment is shown in the inset); and the blue bars represent the seismic moment (Stevens and Avouac (2016) [276]).

Bungum et al. (2017) [43] derived strain rate field along the northwest and the central Himalaya. It varies from 50.09×10^{-9} strain/yr in Kashmir, $61.36 \pm 4.87 \times 10^{-9}$ strain/yr in Himachal, 61.84×10^{-9} strain/yr in Garhwal-Kumaun, 54.59×10^{-9} strain/yr in western and central Nepal, to 57.95×10^{-9} strain/yr in eastern Nepal. In addition, they converted these strain rates into geodetic moment rates and compared the results with seismic moment rates from 115 years of earthquake data where an almost perfect match is found, and with seismic moment rates from 515 years of seismicity data where geodetic moment rates are observed to be higher by a factor of two. The study emphasized higher seismic hazard along the central seismic gap (Fig. 1.8) [43].

Vorobieva et al. (2017) [299] evaluated earthquake cycles and slip deficit rates along various segments of the MFT and found that the seismic cycle varies from 700 years to 2100 years. The slip deficit not only depends on the shortening rate, crustal rheology, and the geological structure but also is influenced by the underneath crustal block. They

observed that decreased seismic activity along the Bhutan Himalaya is controlled by the tectonic motion of the Assam block and the Shillong Plateau [299]. Further, the maximum earthquake potential corresponds to the central seismic gap whereas Kashmir and Assam regions are associated with a lower seismic hazard (Fig. 1.8) [299].

Zheng et al. (2018) [323] utilized an updated GPS velocity field and forecasted required seismicity along the India-Eurasian boundary in terms of 11 events of $M_w \geq 7.5$, 36 events of $M_w \geq 7.0$, 109 events of $M_w \geq 6.5$, or 326 events of $M_w \geq 6.0$ in every 100 years.

Li et al. (2018) [152] integrated GPS data with publicly available data to image the coupling along the MHT and observed that high coupling varies from 100 km to >140 km along the MFT to further north. The observed slip rate of MHT varies from 18.6 ± 1.6 mm/yr, 20.2 ± 1.2 mm/yr, and to 22.2 ± 1.7 mm/yr in the northwest, central, and the northeast Himalaya, respectively. This slip rate builds up as much as strain from the past 300 years to produce a giant $M_w \sim 8.6$ earthquake in the very near future [152].

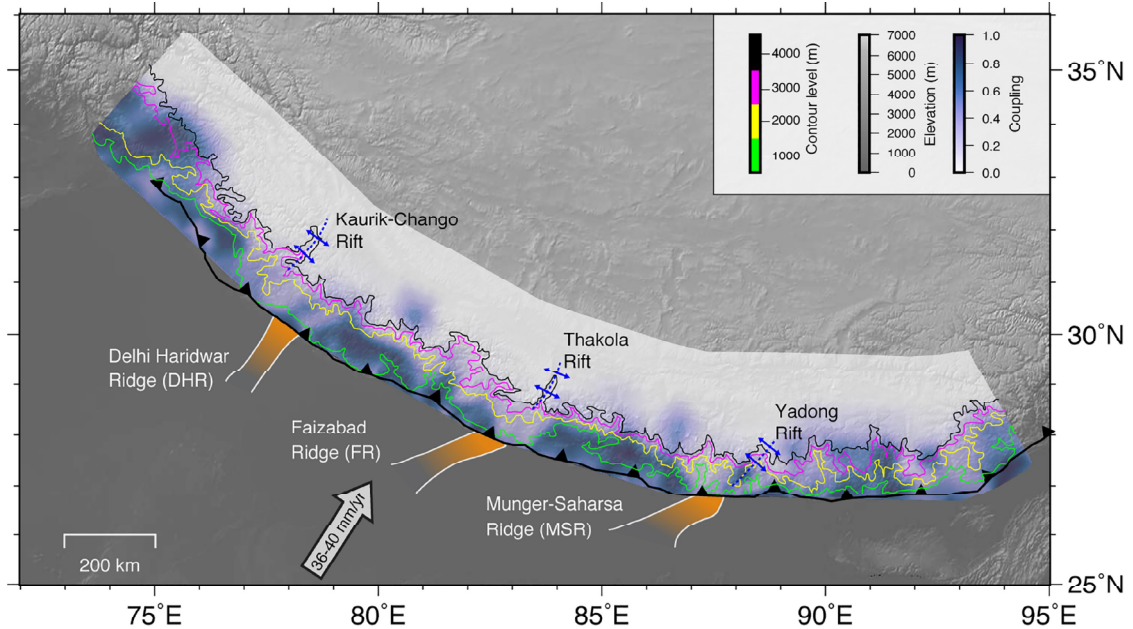


Fig. 2.2: The comparison between interseismic coupling and the Himalayan topography. The blue color indicates fault coupling pattern, whereas the solid color lines represent topographic contour lines. Three arc-normal rifts (KCR, TKR, and YDR) are shown by the dashed lines (Dal Zilio et al. (2020) [62]).

Dal Zilio et al. (2020) [62] compiled GPS, leveling, and InSAR data along the Himalayan arc using a Bayesian framework and found that coupling in the Himalaya is

highly heterogeneous along the MHT (Fig. 2.2). They have also notified lower coupling (a dilated state in which earthquake does not extend through) along the regions between the KCR and the DHR in the northwest Himalaya, the TKR and the FZR in the central Himalaya, and between the YDR and the MSR in the northeast Himalaya (Fig. 2.2) [62].

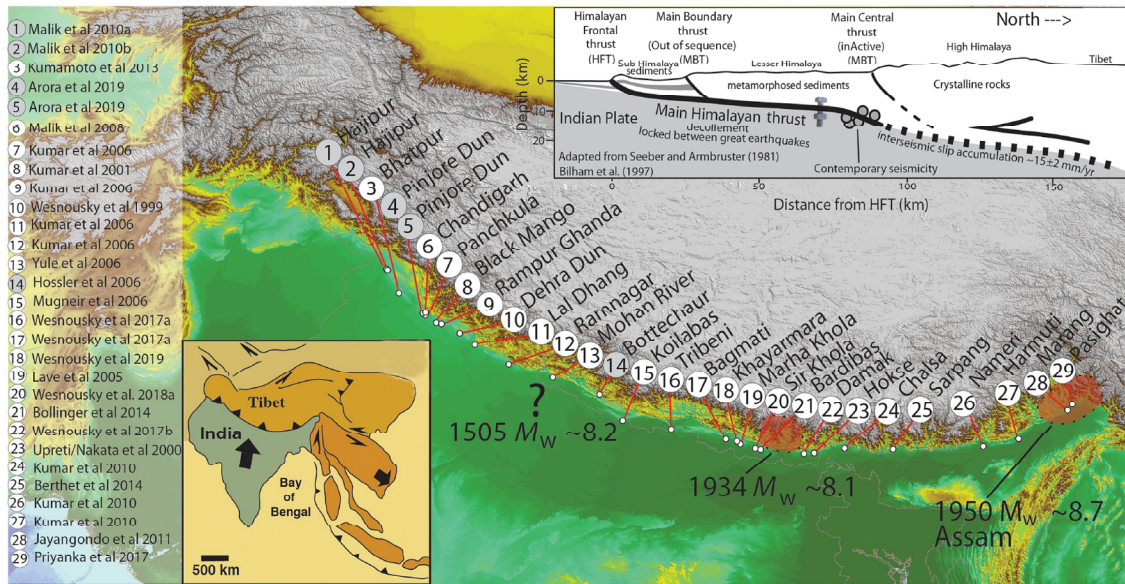


Fig. 2.3: The geological studies of paleoseismic events and slip rate estimation along the MHT. The white circles indicate the locations of the geological studies. The cross-section of the Himalayan arc is shown in the inset (Wesnousky (2020) [305]).

Wesnousky (2020) [305] reviewed all paleoseismic data along the Himalayan orogenic belt in the context of consideration of the temporal variation of great earthquakes (Fig. 2.3). The estimated recurrence period of future great earthquakes ranges from 500–1000 years evaluated from the uplifted scarps, river terraces, and trenching data (Fig. 2.3) [305]. The apparent occurrence of large-sized earthquakes in the past led the author to suggest that the Himalayan arc is poised to produce a sequence of great events near today [305].

Bisht et al. (2020) [38] used six continuous GPS stations along the Himalayan arc. They suggested that the average surface velocity of 46.95 ± 0.23 mm/yr along these stations indicate a northeast directed motion of the Indian plate [38]. They observed a higher eastward velocity (36.11 ± 0.17 mm/yr) than the northward velocity (29.02 ± 0.16 mm/yr) [38]. They computed 8.06 ± 0.28 mm/yr of convergence rate along the Higher Himalaya and 5.71 ± 0.17 mm/yr of convergence rate along the Lesser Himalaya [38]. Using a baseline model, they estimated 11.68 ± 1.32 mm/yr of shortening above the MCT and $6.74 \pm$

mm/yr of shortening above the MBT with respect to the Indian plate [38]. Similarly, with respect to the Eurasian plate, they estimated 20.60 ± 1.76 mm/yr shortening above the MCT and 11.42 ± 1.21 mm/yr of shortening above the MBT [38]. From the above shortening rates, they suggested that sufficient maximum strain is accumulated along the region between the MCT and the MBT to produce a large-sized event [38].

Saji et al. (2020) [248] analyzed crustal deformation related to the hydrological mass variations along the Indian plate using a set of 50 GPS stations and Gravity Recovery and Climate Experiment (GRACE) observations during 2004–2015. They suggested that the Siwalik and the IGP are currently subsiding, whereas the adjacent regions show upliftment [248]. Further, they estimated 12.40 ± 2.01 mm/yr of slip rate along the MHT [248].

Apart from the above large scale studies, the following sections present several important geological and geodetic studies along the three broader segments of the Himalayan arc.

2.3 Seismic hazard along the northwest Himalaya

The northwest Himalaya is considered to be one of the most interesting segments to study active tectonics along the Himalayan arc [60]. The majority of crustal strain accumulation along this region is accommodated by the mainstream thrust system of the Himalayan belt [195]. This arcuate thrust system had evolved during the late Tertiary to mid-Quaternary period as a consequence of the persistent tectonic collision between India and Eurasia plates at an average rate of $\sim 4\text{--}5$ cm/yr [283, 321].

2.3.1 Geological studies along the northwest Himalaya

Below the geological studies along the northwest Himalaya are organized based on their trenching locations (Fig. 2.4).

¹Vassallo et al. (2015) [296] determined Late-Quaternary shortening rate of 11.2 ± 3.8 mm/yr and 9.0 ± 3.2 mm/yr for MWT and MFT, respectively. This implies a total long-term shortening rate for the MHT as $13.2\text{--}27.2$ mm/yr (Fig. 2.4).

Utilizing carbon dating along fluvial terraces in the Kangra reentrant, ²Vignon et al. (2017) [298] found that the MWT has a constant long-term vertical uplift of 10.6 ± 2.0 mm/yr, suggesting the occurrence of a number of large earthquakes along this fault. The 2005 Kashmir earthquake was one of such events.

³Gavillot et al. (2016) [89] mapped active faulting along the Kashmir Himalaya, near the rupture zone of the 2005 Kashmir earthquake (Fig. 2.4). Using the age data and structural analysis of sedimentary rocks along the Raisi fault (a splay fault of MFT), they observed that their study region falls into a seismic gap (known as Kashmir seismic gap), which has the potential of a larger earthquake than the 2005 Kashmir event [89].

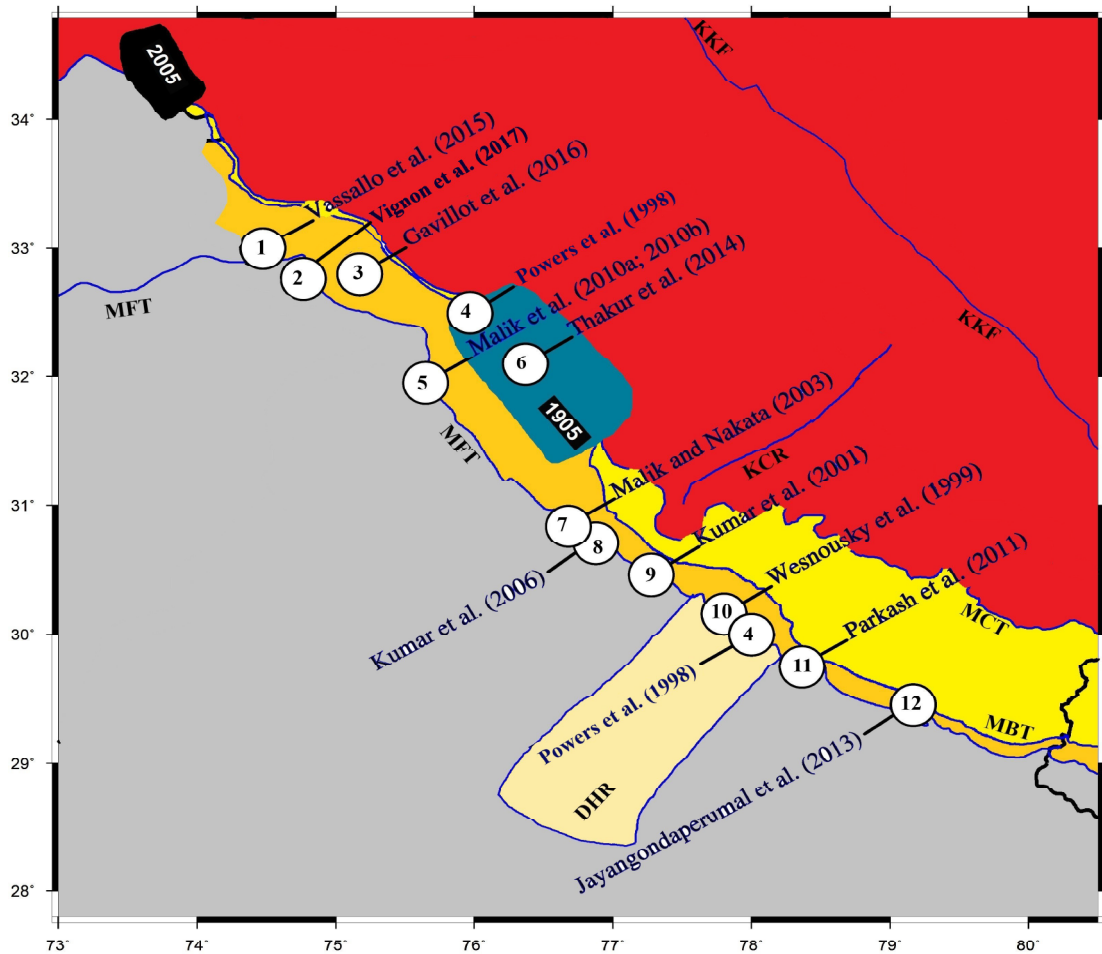


Fig. 2.4: Geological studies along the northwest Himalaya. Abbreviations are as follows: DHR, Delhi-Haridwar Ridge; KCR, Kaurik Chango Rift; KKF, Karakorum Fault; MBT, Main Boundary Thrust; MCT, Main Central Thrust; MFT, Main Frontal Thrust.

⁴Powers et al. (1998) [223] estimated the late Neogene shortening rate of the MFT in the Kangra reentrant and the Dehradun reentrant as 14 ± 2 mm/yr and 6–16 mm/yr,

respectively. They also suggested that the south verging thrust system along the sub-Himalaya roots into a 2.5° – 6.0° northward dipping décollement [223]. With a continuous large shortening rate (14 ± 2 mm/yr), the Kangra reentrant is likely to host moderate to great earthquakes in the near future [223].

⁵Malik et al. (2010a, 2010b) [162, 164] utilized Ground Penetrating Radar (GPR) data across two fault scarps of MFT (named as Hajipur Fault; HF1 and HF2) in the northwestern end of the Janauri anticline and observed that with a slip rate of 7.6 ± 1.7 mm/yr, uplift rate of 3.2 ± 0.6 mm/yr, and shortening rate of $\sim 6.9 \pm 1.4$ mm/yr, the MFT is capable to generate a large earthquake ($M_w \geq 7.0$) with a recurrence interval of 1160 ± 250 years [162, 164].

⁶Thakur et al. (2014) [283] acquired radiocarbon dating of fluvial terrace deposits along the Kangra reentrant in one seismic profile and observed the long-term slip rates of the MFT, JMT, ST (Soan Thrust), and the back thrust of Janauri anticline as ~ 6.9 mm/yr, and ~ 4.2 mm/yr, ~ 3.0 mm/yr, and ~ 2.2 mm/yr, respectively (Fig. 2.4). They have also suggested that large earthquakes like the 1905 Kangra ($M_w=7.8$) event and the 2005 Kashmir ($M_w=7.8$) event or great to mega-earthquakes could propagate through the Himalayan front [283].

⁷Malik and Nakata (2003) [161] investigated preliminary trenches and fault scarps due to a large historical event near Pinjore Dun (near Chandigarh) along the MFT (Fig. 2.4). Taking into account the age of fault scarp as 50 Ka to 10 Ka and the vertical displacement of 20 m to 25 m along the Pinjore Dun, they have estimated $\sim 6.3 \pm 2.0$ mm/yr of slip rate and 5.8 ± 1.8 mm/yr of shortening rate along the 25° dipping MFT. This slip rate of the MFT is capable of generating another large event with a recurrence interval of 555 ± 118 years [161].

⁸Kumar et al. (2006) [138] analyzed the quaternary expression of rupture area due to a great historical earthquake along a 250 km long stretch along the strike of the MFT. They obtained a vertical uplift rate of ~ 4 – 6 mm/yr on $\sim 20^\circ$ – 45° dipping MFT. This rate is equivalent to a slip rate of ~ 6 – 18 mm/yr and a shortening rate of ~ 4 – 16 mm/yr. They also suggested the possibility of a massive earthquake larger than recorded historically based on the evidence from fault scarps and displacement along the fluvial terrace deposits along the MFT (Fig. 2.4) [138].

⁹Kumar et al. (2001) [142] investigated that the Black Mango Fault (BMF), a branch of the MFT, displays evidence of two great Himalayan earthquakes around 650 years ago. Terraces along the Markanda river show uplift of $\sim 4.8 \pm 0.9$ mm/yr due to the underlying

MFT [142]. This uplift is equivalent to a slip rate of $\sim 9.6 \pm 3.5$ mm/yr and shortening of $\sim 8.4 \pm 3.6$ mm/yr for the $\sim 30^\circ \pm 10^\circ$ dipping MFT [142].

¹⁰Wesnousky et al. (1999) [310] carried out radiocarbon dating of fluvial terrace deposits along a 40 km stretch of the MFT near the Dehradun region (Fig. 2.4). They reported that the horizontal shortening rate along the Dehradun region is $\sim 11.9 \pm 3.1$ mm/yr and the slip rate of MFT is $\sim 13.8 \pm 3.6$ mm/yr. This indicates a potential for a destructive earthquake in the Dehradun region [310].

¹¹Parkash et al. (2011) [210] have performed carbon dating of sediments along four terraces of the river Ganges in Haridwar close to the MFT (Fig. 2.4). The results suggest an overall vertical displacement of $\sim 6.23 \pm 1.29$ mm/yr along with a slip rate and shortening rate of 12.46 ± 2.58 mm/yr and 10.79 ± 2.23 mm/yr, respectively [210].

¹²Jayangondaperumal et al. (2013) [117] analyzed two trenching sites across MFT in Garhwal-Kumaun Himalaya where they observed that two great events before 1400 AD have occurred and a magnitude ~ 8.5 earthquake is still waiting to release the remaining seismic energy in the near future (Fig. 2.4).

Based on the above geological studies, it is observed that the slip rate of MFT varies between 6.3 mm/yr and 14.0 mm/yr from the Kashmir Himalaya to the Kumaun Himalaya. The above studies also suggest that the northwest Himalaya has stored sufficient strain energy to produce a great earthquake with a recurrence period of 500–1000 years.

2.3.2 Geodetic studies along the northwest Himalaya

Since 1995 [20], there have been several geodetic studies along the northwest Himalaya to understand the present-day crustal deformation and associated earthquake potential in this region. Moreover, it has been observed that the GPS measured displacement rates in the interseismic period often complement the long-term crustal deformation estimates from paleoseismic or geomorphic studies. The below section highlights some of the geodetic studies.

In the Western Himalaya, the first GPS network comprising 26 campaign sites was established in 1995 across the rupture zone of the 1905 Kangra earthquake and the western portion of the adjoining seismic gap segment [20]. Banerjee and Bürgmann (2002) [20] estimated 11 ± 4 mm/yr of slip rate for the Karakorum Fault (KKF) and observed that this fault slip of KKF contributes to the east-west extension of the southern Tibet and the westward motion of the northwestern Himalaya towards Nanga Parbat. Crustal locking of ~ 100 km was observed along the Siwalik Himalaya to further north with a slip deficit

rate of 14 ± 1 mm/yr along the MFT. They suggested that the estimated accumulated slip will eventually release in great Himalayan earthquakes [20].

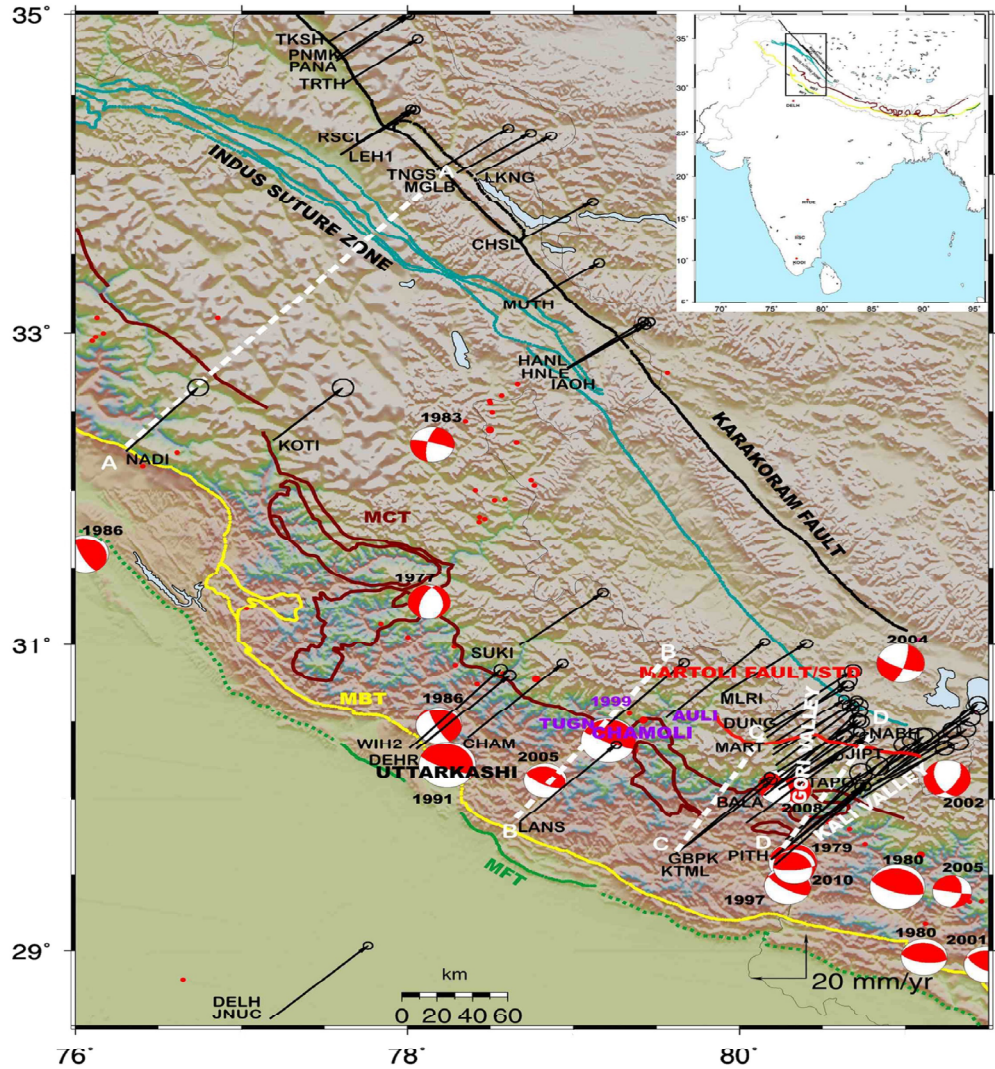


Fig. 2.5: Surface velocity field along the northwest Himalaya. Beach balls represent focal mechanism of the past earthquakes of magnitude $M_w \geq 5.0$ and focal depth ≤ 50 km (Jade et al. (2014) [114]).

Jade (2004) [110] and Jade et al. (2004) [111] estimated convergence between the Indian subcontinent and the Tibetan Plateau as 14–20 mm/yr, and the convergence rate in the Garhwal Himalaya to be 10–18 mm/yr. Further, Jade et al. (2011) [115] re-estimated deformation rates in Ladakh using 11 years of GPS data accrued from two permanent and eight campaign stations across the KKF (Fig. 2.5). They obtained a movement of 32–34 mm/yr for all Ladakh sites and a dextral slip of 3 mm/yr for the KKF (Fig. 2.5) [115]. A

comprehensive summary of horizontal velocities, convergence, and extension rates of 14 permanent and 42 campaign GPS stations along the northwest Himalaya is provided by Jade et al. (2014) [114]. They reported that the surface velocities vary between 30–48 mm/yr and the arc-normal shortening rate varies between 10–14 mm/yr along different transects of the northwest Himalayan wedge (Fig. 2.5) [114]. They have also reported slip rate, dip angle, and locking width of the MHT as 16 ± 1 mm/yr, 5° , and 109 km, respectively in the Garhwal region and 18 ± 1.5 mm/yr, 8° , and 110 km, respectively in the Kumaun Himalaya (Fig. 2.5) [114]. Recently, Jade et al. (2020) [112] presented a horizontal velocity field along Kashmir and its surrounding regions from a dense network of continuous GPS stations from 2008 to 2019 (Fig. 2.5). They computed ~ 16 mm/yr of oblique slip rate of the MHT at a locking depth of ~ 15 km and a width of ~ 145 km along the Kashmir Himalaya. They observed ~ 7 mm/yr of lengthening in this region. They suggested that the long-term stored strain energy and microseismic activity along the Kashmir seismic gap indicate the possibility of a $M_w \sim 7.7$ earthquake in the near future [112].

From a combination of GPS data and aftershock distribution of the 2005 Kashmir earthquake, Bendick et al. (2007) [24] obtained a geodetic convergence rate of 7 ± 2 mm/yr between Peshawar, Leh, and Ladakh. They suggested that the 2005 Kashmir type earthquake has a recurrence interval of 680 ± 150 years [24].

Reddy and Prajapati (2009) [232] monitored postseismic deformation of the 2005 Kashmir earthquake for about a year using three continuous GPS stations at Gulmarg, Amritsar, and Jaipur. A higher horizontal velocity of 8.6 cm/yr at Gulmarg than the station velocities at Amritsar (5.9 cm/yr) and Jaipur (5.1 cm/yr) suggests that the postseismic transients near the source of the 2005 event are probably caused due to an afterslip or viscous relaxation [232].

Geodetic strain field analysis and slip rate distribution beneath the northwest Himalaya were carried out by Ponraj et al. (2010, 2011, 2019) [219, 220, 221] using three years of measurements from 16 campaign sites (Fig. 2.6). Ponraj et al. (2010) [221] estimated 41–50 mm/yr horizontal velocity for all GPS stations. They observed that ~ 15 mm/yr convergence rate is accommodated within the Kumaun Himalaya [221]. The authors noticed that large dilatational strain rates as well as maximum shear strain rates are accommodated along the MCT in this region [221]. Further, Ponraj et al. (2011) [220] estimated a slip rate of 10 mm/yr of the MHT beneath the northwest Himalaya (Fig. 2.6). In addition, their analysis from the Non-Uniform Creep (NUC) dislocation

model suggests a locking depth of ~ 15 km in the northwest Himalaya [220]. They concluded that the deformation is concentrated between the Lesser Himalaya and the Higher Himalaya and suggested the presence of structural discontinuity on the fault between the Kumaun and Garhwal Himalaya [220]. Ponraj et al. (2019) [219] re-calculated slip rate of $\sim 17.2 \pm 1.0$ mm/yr and locking depth (~ 20 km) along $\sim 7^\circ$ dipping MHT in the Kumaun Himalaya using a NUC dislocation model (Fig. 2.6). The slip rate of the MHT corresponding to a moment deficit rate of $8.4 \pm 1.0 \times 10^{18}$ Nm/yr indicates the possibility of a great earthquake ($M_w \geq 8.0$) with a return period of 600 years in the Kumaun region [219].

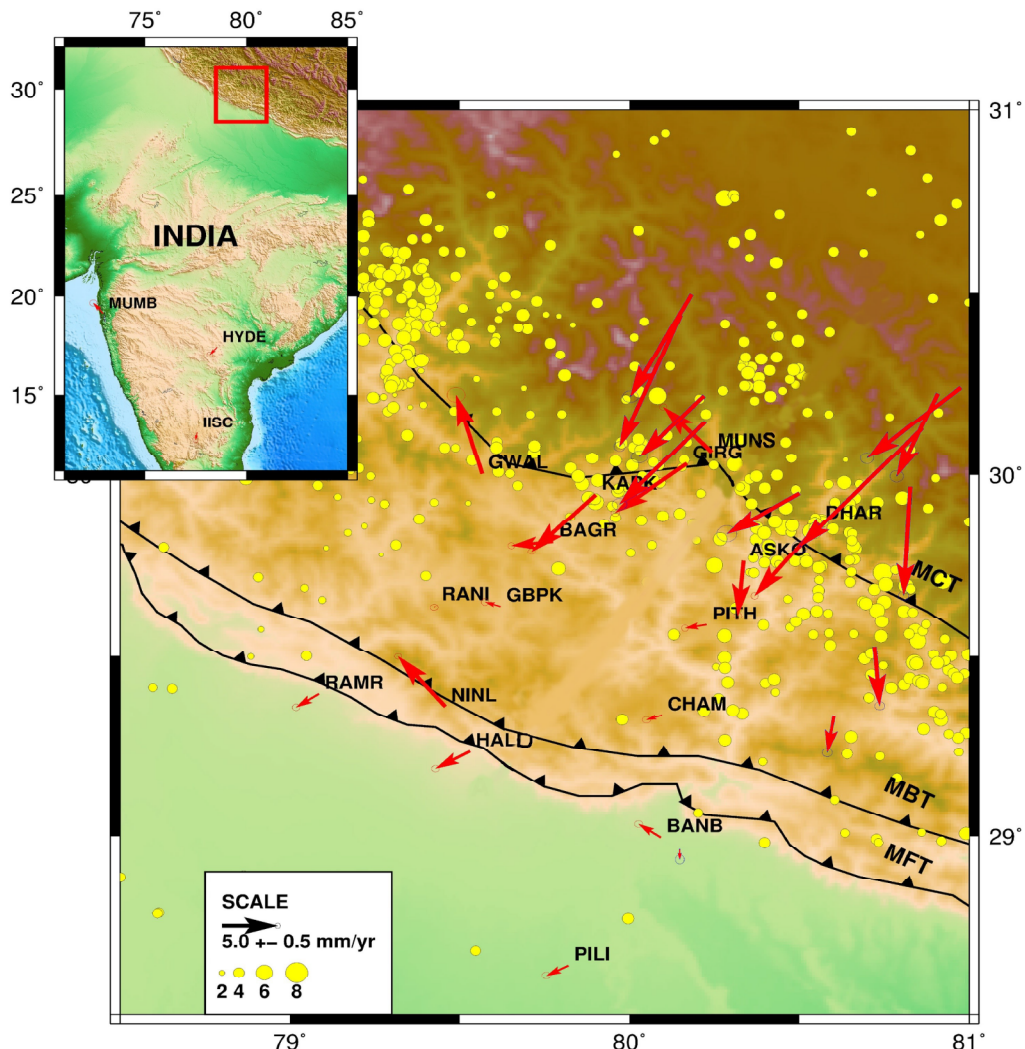


Fig. 2.6: Surface velocity field and seismicity along the Kumaun Himalaya. The red arrows represent GPS velocity vectors and the yellow circles indicate seismicity since 1911 (Ponraj et al. (2019) [219]).

Schiffman et al. (2013) [254] obtained 11 ± 1 mm/yr geodetic slip rate of the MHT along with a dextral motion of 5 ± 1 mm/yr. With an estimated slip rate of 4 ± 2 mm/yr, the MFT is locked up to 170 km from its surface location to further north in the Kashmir Himalaya [254].

Kundu et al. (2014) [143] have recorded horizontal GPS signals in the Kashmir Himalaya and noticed 17 ± 2 mm/yr of oblique convergence, which is partitioned into 5 ± 2 mm/yr of strike-slip motion and 13.6 ± 1.0 mm/yr of arc normal motion. They have also suggested that the Kaurik Chango Rift (KCR) is a seismically active rift, which may propagate up to the MFT and can probably arrest the propagation of large rupture along the northwest Himalaya [143].

Crustal deformation in Kumaun Himalaya was studied by Dumka et al. (2014) [68] from 25 GPS observations (2003–2006) along two transects. Their analysis revealed that the MFT and the MBT are currently locked, whereas the MCT indicates maximum deformation rates [68]. A horizontal shortening of 6.7 ± 2.5 mm/yr is observed between the Lesser Himalaya and the IGP [67]. Further, Dumka et al. (2018) [69] re-calculated slip rates of the MFT, MBT, and the MCT. They observed 1.5 ± 1.0 mm/yr slip rate for the MFT, 5.2 ± 1.2 mm/yr slip rate for the MBT, and 8.7 ± 1.7 mm/yr slip rate for the MCT. They estimated high rates of compression and shear strain along the MCT. They suggested that the shallow to the down-dip edge of the MHT is fully locked.

Yhokha et al. (2015) [318] presented InSAR images of the Nainital region and observed that the G-KF divides the lower Kumaun Himalaya into two different segments with an uplift in the west and a subsidence in the east (Fig. 1.5). Further, in 2018, Yhokha et al. [319] utilized the Persistent Scatterer Interferometry (PSI) technique to understand and monitor the slope movements in the Nainital region of the Kumaun Himalaya. Using a total of 15 SAR images, they observed a continuous creeping of ~ 21 mm/yr at hilltop and ~ 5 mm/yr of creeping at the downslope in the eastern side of Nainital lake along the Kumaun Himalaya [319].

Using InSAR and GPS observations along the Tehri Dam in Garhwal region, Gahalaut et al. (2017) [85] have found evidences of large subsidence in this region. The subsidence due to filling cycles of the reservoir of the Tehri Dam is consistent with the annual modulation in the vertical and north components of the time-series of continuous GPS stations [85].

Gautam et al. (2017) [88] evaluated ~ 18 mm/yr slip rate of the MHT over a ~ 100 km locked portion in the Garhwal-Kumaun Himalaya based on the observations from five

continuous GPS stations in the region (Fig. 2.7). They suggested that the stored strain budget over the past 500–700 years is sufficient to produce a great earthquake along the Garhwal-Kumaun Himalaya [88].

Sharma et al. (2018) [264] have utilized 23 GPS stations along the Garhwal-Kumaun Himalaya. Using a 2D inversion model, they estimated insignificant (~ 1 mm/yr) slip rate and 22° dip angle for the MFT in this region. They observed large variation (2–16 mm/yr) in the arc-normal motion from the MFT to further north [264].

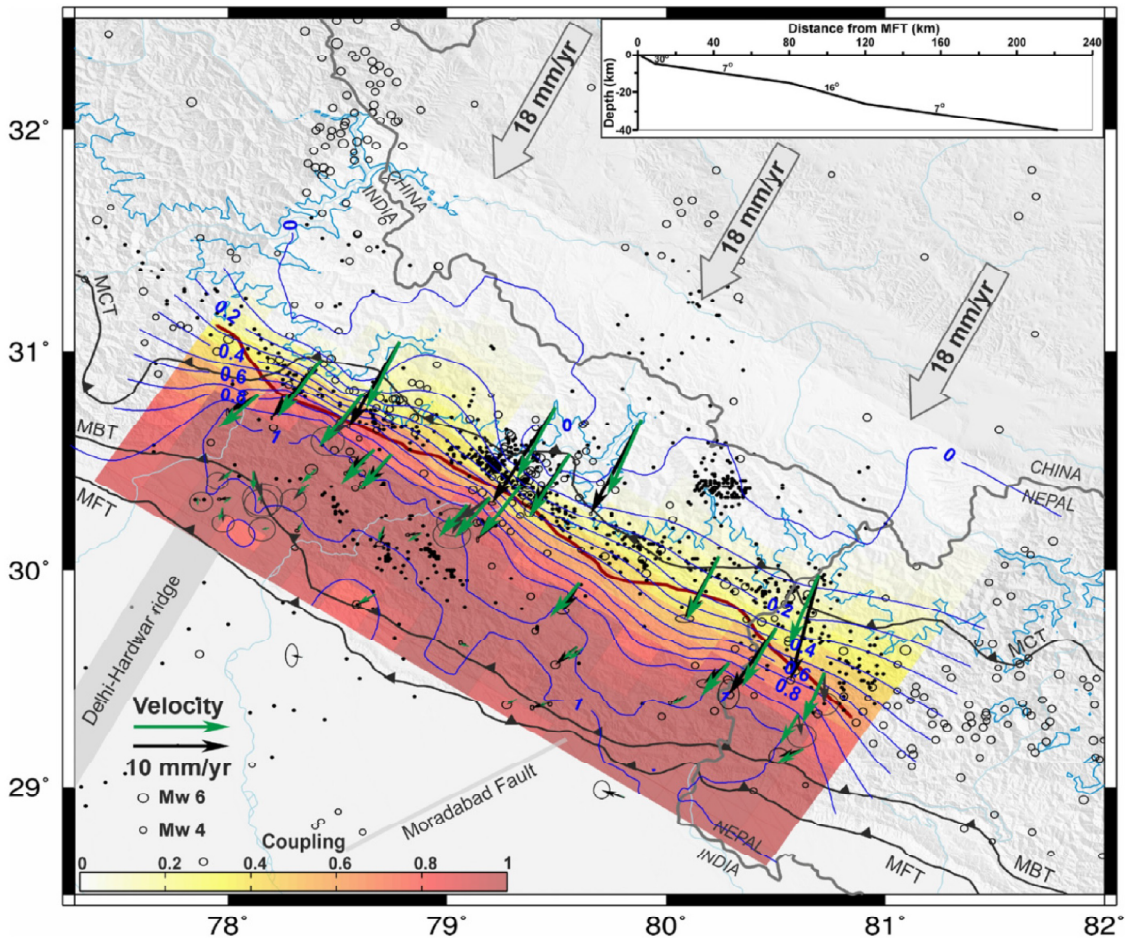


Fig. 2.7: Interseismic coupling map of the northwest Himalaya. The blue lines indicate coupling contours; the black arrows show the observed GPS velocity vector; and the green arrows represent the simulated velocity vector (Yadav et al. (2019) [316]).

Using 28 GPS stations, Yadav et al. (2019) [316] computed strong seismic coupling of 85 km in the Garhwal-Kumaun Himalaya along the MHT (Fig. 2.7). They observed a slip rate of 18 mm/yr of MHT at a depth of ~ 20 km (Fig. 2.7). They remarked that

the coupling in the Outer and Lesser Himalaya is homogeneous and is not influenced by the DHR (Fig. 2.7) [316]. The accumulated strain along the fully locked MHT in the last \sim 500 years lists the northwest Himalaya among the highly seismic hazardous regions of the world (Fig. 2.7) [316]. Further, Yadav et al. (2020) [315] computed a larger compression strain rate of $\sim -0.15 \mu$ strain/yr along the upper Kumaun Himalaya, whereas, along the lower Kumaun Himalaya, they have found two strongly coupled zones (Fig. 2.7). This discontinuity represents deformation heterogeneity along the Kumaun Himalaya [315]. They argued that the region with higher strain accumulation rates and strong coupling is the most likely zone to produce future large earthquakes (Fig. 2.7) [315]. They suggested that the Kumaun Himalaya has stored sufficient strain energy equivalent to a great earthquake of $M_w \sim 8.2$ [315].

Sharma et al. (2020) [261] have used nine GPS stations along the Garhwal-Kumaun Himalaya. They estimated 0.1–2.0 mm/yr slip rate along the MFT, indicating its locking behavior. They observed that this insignificant slip rate of MFT leads to strain energy accumulation which will release through future earthquakes [261].

From the above literature, it is observed that the MFT shows an insignificant slip rate along the entire northwest Himalaya, indicating its locking behavior. The locking zone varies from \sim 170 km in the Kashmir Himalaya to \sim 110 km in the Kumaun Himalaya. In addition, oblique plate motion is also observed along the Kashmir Himalaya. It was noted that the slip rate of the MHT varies from \sim 11 mm/yr along the Kashmir valley to \sim 18 mm/yr along the Kumaun region. Nonetheless, all of the above geodetic studies indicate that the strain accumulation along the northwest Himalaya is equivalent to a great earthquake with a return period of 500–700 years.

2.4 Seismic hazard along the central Himalaya

Situated in one of the most seismically active continental collision orogenic belts of the world, the central Himalaya has witnessed a series of devastating earthquakes in the past [30, 180]. Geological and geodetic studies indicate that one or more moderate to great earthquakes are overdue along this region [2, 154, 305]. Thus, a thorough understanding of the crustal processes and the study of previous large to great earthquakes in the central Himalaya would provide an improved hazard mitigation strategy and preparedness along the densely populated central Himalayan region. Below a summary of some geological and geodetic studies in the central Himalaya is provided.

2.4.1 Geological studies along the central Himalaya

The geological studies along the central Himalaya are discussed below from west to east based on their trenching locations (Fig. 2.8).

¹Rajendran et al. (2018) [228] found that a great earthquake of $M_w \geq 8.5$ occurred in the central Himalaya, possibly in 1505 AD. The event produced a fracture of about 600 km with an average slip of 15 m. Considering a recurrence interval of ~ 700 years, they suggested that a similar magnitude earthquake is probably overdue in the central Himalayan segment (Fig. 2.8).

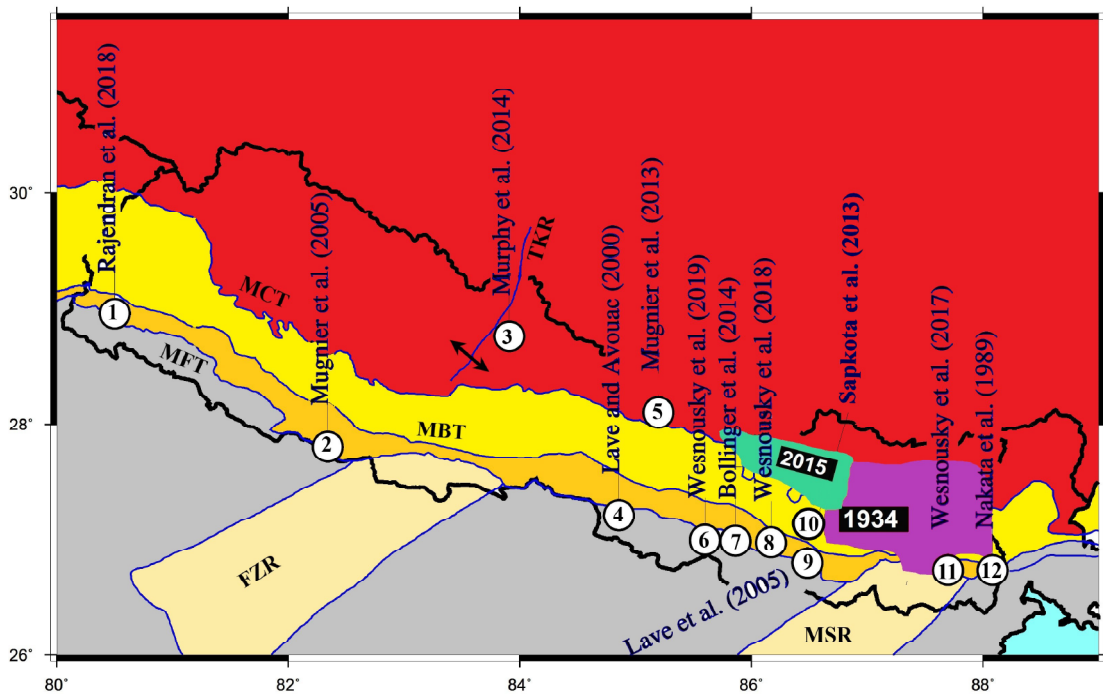


Fig. 2.8: Geological studies along the central Himalaya. Abbreviations are as follows: FZR, Faizabad Ridge; MBT, Main Boundary Thrust; MCT, Main Central Thrust; MFT, Main Frontal Thrust; MSR, Munger-Saharsa Ridge; TKR, Thakola Rift.

²Mugnier et al. (2005) [180] studied an uplifted scarp of about 8 m along the MFT in the western Nepal. Based on their findings, they suggested that this scarp is formed due to two historical events of $M_w \sim 8.0$ between 1224–1280 AD and between 1828–1883 AD, respectively (Fig. 2.8). They have reported that such surface rupture along the MFT has a return period of ~ 700 years in this region [180]. They found that during the Holocene period, the MFT was active with a persistent slip rate of 19 ± 6 mm/yr, though, its splayed

piggyback thrust (MDT) showed episodes of activity from a few meters to tens of meters of deformation [180, 182].

³Murphy et al. (2014) [190] used radiocarbon dating to test the sedimentary rock of a 10 m uplifted scarp on the MFT in the western Nepal and concluded that this scarp is created during one or more great events in 1165–1400 AD (Fig. 2.8).

⁴Lave and Avouac (2000) [145] analyzed geomorphic evidences of crustal deformation from terraces of Bagmati and Bakeya rivers along the frontal part of the central Himalaya (Fig. 2.8). Here the uplifted displacement of 1.5 cm/yr, derived from river incision, implies a long-term slip rate of 21 ± 1.5 mm/yr along the MFT. They found that the MFT is locked in the interseismic period and will eventually release the accumulated strain through large ($M_w > 8.0$) earthquakes in the near future [145].

⁵Mugnier et al. (2013) [179] combined data from historical archives, trenches along surface ruptures of past large events, isoseismal damage mapping, seismites, and instrumental seismicity records along Kathmandu to understand an open question: “Does a great earthquake (like 1934 Nepal Bihar earthquake of magnitude $M_w=8.1$) release all the interseismically stored strain or does it also release the background strain, which remained unreleased through earlier historical earthquakes?” Based on the findings, they remarked that the Himalayan giant earthquakes have a dynamic deformation pattern as well as a dynamic recurrence interval. In other words, they suggested that the Himalayan earthquakes exhibit space-time randomness and thus the next giant earthquake ($M_w \geq 8.6$) can occur anywhere along the central Himalaya [179].

⁶Wesnousky et al. (2019) [306] studied 7 m uplifted scarp along MFT due to a historical event in 1050–1200 AD at Khayarmara site, ~80 km southwest of Kathmandu (Fig. 2.8). However, there were no evidences of surface rupture at that site due to the 1934 event. With a recurrence interval of >700 years, their study suggests that there is a possibility of a great earthquake in this region [306].

⁷Bollinger et al. (2014) [40] constrained late Holocene return period between 750 ± 140 years to 870 ± 350 years for great Himalayan earthquakes along $25^\circ \pm 5^\circ$ N dipping MFT in the eastern Nepal. They have computed slip rates of two branching faults of the MFT, namely the Patu thrust and the Bardibas thrust, as 8.5 ± 1.5 mm/yr and 11 ± 1 mm/yr, respectively (Fig. 2.8) [40].

Using paleoseismic investigation, ⁸Wesnousky et al. (2018) [309] reported rupture zone of the 1934 Nepal-Bihar earthquake. They suggested that the MFT was not the

source fault for this event, indicating that the MFT remains undeformed during the interseismic period (Fig. 2.8).

⁹Lave et al. (2005) [146] presented paleoseismic evidences from trenching along the central Himalaya (Marha Khola in eastern Nepal) and observed that only a single event occurred in history probably in \sim 1100 AD. This event had ruptured MFT with a lateral extent of \sim 250 km and a magnitude of $\sim M_w=8.8$. They suggested that such an event would return in 1800–3000 years (Fig. 2.8).

From the paleoseismic trenching and geomorphic imaging of the sedimentary deposits along the river cliffs in the eastern Nepal, ¹⁰Sapkota et al. (2013) [251] showed that the 1934 Nepal-Bihar earthquake has provided surface rupture of \sim 150 km along the MFT. They observed that two great events in 1255 AD and 1934 AD have ruptured along the eastern Nepal and largely contributed to the upliftment of river terraces along the MFT [251]. Apart from these earthquakes, they also suggested that other historically blind great Himalayan earthquakes might exist along the eastern Nepal [251].

¹¹Wesnousky et al. (2017) [308] examined structural and radiocarbon observations of a 11.3 ± 3.5 m dip-slip displacement that occurred due to a great event in 1146–1256 AD along the MFT near Damak in the eastern Nepal Himalaya and noticed that sufficient strain is accumulated along the MFT to produce a similar great earthquake with a recurrence interval of \sim 800 years (Fig. 2.8).

¹²Nakata (1989) [191] collected sedimentary rock samples and areal photographs to study the active faulting along the central Himalaya (Fig. 2.8). The observed average uplift of \sim 3–4 mm/yr and strike-slip of \sim 1.2 mm/yr along the Himalayan front indicate \sim 5 mm/yr of dip-slip motion along the MFT [191].

The above geological studies suggest that many blind great Himalayan earthquakes with a return period of 700–900 years have ruptured along the central Himalaya since \sim 1100 AD. It has been reported that the long-term slip rate of the MFT varies from \sim 7 mm/yr to \sim 21 mm/yr, sufficient to produce great earthquakes along the central Himalaya.

2.4.2 Geodetic studies along the central Himalaya

In the Nepal-Himalaya, the first GPS-based research related to the India-Tibet convergence was initiated by Bilham et al. (1997) as early as in 1991. Bilham et al. (1997, 1998) [32, 35] utilized six years of GPS measurements to derive slip rate of the MHT. The slip rates are 20.5 ± 2.0 mm/yr in the western Nepal and 21 ± 3 mm/yr in the central and eastern Nepal. This estimated slip rate of MHT suggests that parts of the arc where

no great event occurred in the last 300 years, such as the western Nepal, have a higher chance to experience one [32, 35].

Larson et al. (1999) [144] evaluated 18 ± 2 mm/yr of contraction rate along the western Nepal using a 2D dislocation model. The dip-slip rate of the MHT was obtained as 23 ± 2 mm/yr and 21 ± 1 mm/yr with 8° dip angle and 112° strike angle in the western Nepal and 3° dip angle and 101° strike angle in the eastern Nepal, respectively [144].

Bürgmann et al. (1999) [45] proposed a segmented fault model for the Nepal Himalaya and suggested an along-the-arc variation in the convergence process. GPS models for varying dip angles (3° – 8°) revealed a locking depth of 15–25 km. They concluded that at least a ~ 500 km long stretch of the fault system with a width of about 140 km is locked, which in turn has produced 6–15 m of accumulated potential slip since the 1505 earthquake [45]. This indicates that this part of the Himalayan orogeny is ready to trigger one or more future great earthquakes [45]. They observed that the short-term geodetic slip of 20 ± 2 mm/yr was consistent with the long-term geological rate of 21.0 ± 1.5 mm/yr deduced from the folded terraces across the Siwalik Hills in the central Nepal Himalaya [45].

Chen et al. (2004) [50] used GPS data from 33 sites to study ongoing crustal deformation along Nepal and southern Tibet. The reported 13 ± 2 mm/yr of elongation rate along the southern Tibet is composed of 9.7 ± 3.0 mm/yr of permanent extension and ~ 3 mm/yr of elastic deformation along the locked MHT [50]. Apart from this, they computed slip rate of the décollement (MHT) as 17 ± 1 mm/yr, 12.4 ± 0.4 mm/yr, and 19 ± 1 mm/yr along the northwest, central, and the northeast Himalaya, respectively [50].

Jouanne et al. (2004) [124] characterized fault parameters by applying a 2D dislocation model on the velocity field from 35 GPS sites in Nepal. In the western Nepal, 117° striking MHT revealed 19 mm/yr of dip-slip and 0–1 mm/yr of strike-slip at 20–21 km depth [124]. In the central Nepal, 108° striking MHT revealed 19–20 mm/yr of slip rate and 0–2 mm/yr of dextral motion at 17–21 km depth [124]. Consequently, the larger locking width in the western Nepal than that of the central Nepal indicates a higher possibility of $M_w > 8.0$ earthquake in this region [124].

Bettinelli et al. (2006) [26] used GPS and DORIS measurements to determine deformation pattern along the western Nepal and observed a slip rate of MHT as 13.4 ± 5.0 mm/yr with a locking width of 150 km. Similarly, they calculated 19.0 ± 2.5 mm/yr slip rate for MHT and 115 km of locking width at about 20 km depth in the central and the eastern Nepal regions [26].

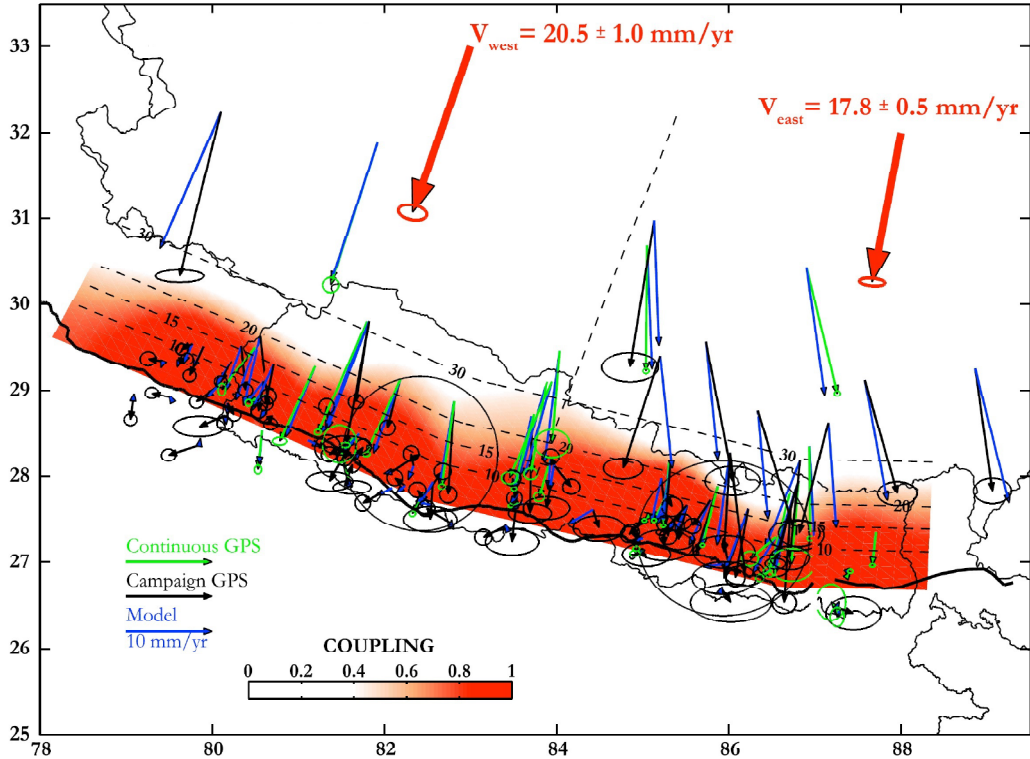


Fig. 2.9: Interseismic coupling map of the central Himalaya (in shaded red color). The green and black arrows indicate continuous and campaign GPS velocity vectors, respectively. The blue arrows represent simulated velocity vectors. The black dashed lines show contour lines of the fault depth (Ader et al. (2012) [2]).

Ader et al. (2012) [2] estimated slip rate of 10° dipping MHT as $17.8 \pm 0.5 \text{ mm/yr}$ in the central and the eastern Nepal, and $20.5 \pm 1 \text{ mm/yr}$ in the western Nepal (Fig. 2.9). They suggested that the western Nepal has not ruptured since the 1505 earthquake and a large moment deficit is accumulated between the 1934 Bihar-Nepal earthquake and the western border of Nepal. As a result, this region may generate an earthquake of up to $M_w \sim 8.9$ [2]. They estimated the transition zone between the fully locked and the aseismic creeping portion of the MHT and found that this zone coincides with the belt of the mid-crustal microseismicity underneath the Himalaya (Fig. 2.9) [2]. They concluded that the background seismicity does not contribute much to release interseismic stress build-up but it does reflect areas of most rapid stress increase [2]. Finally, they observed that the estimated slip rate of MHT represents the moment deficit rate of $6.6 \pm 0.4 \times 10^{19} \text{ Nm/yr}$ underneath the central Himalaya (Fig. 2.9) [2]. This moment deficit rate is equivalent to a great earthquake of $M_w \sim 8.5$ with a recurrence interval of ~ 270 years [2].

Grandin et al. (2012) [91] utilized InSAR data to measure the long-term growth and crustal deformation in the central Nepal and reported that the frontal part (i.e. along MFT) of the Himalayan range is uplifting at a rate of 7 mm/yr. The flat of the décollement (i.e., MHT) is slipping with a rate of 18–21 mm/yr, though the mid-crustal ramp of the décollement is fully locked in the Higher Himalayan part (Fig. 1.4) [91].

Li et al. (2016) [153] calculated locking depth and slip deficit rate along the MHT as 12–17 km and 0–5 mm/yr along the western Nepal, 16–21 km and 6–10 mm/yr along the central Nepal, and 23–26 km and 8–13 mm/yr along the eastern Nepal. They noticed that the 2015 Gorkha event created a boundary in between the western and central Nepal where the slip deficit rate changes significantly from 0 to 9 mm/yr, causing a high strain accumulation in the central and the eastern part [153].

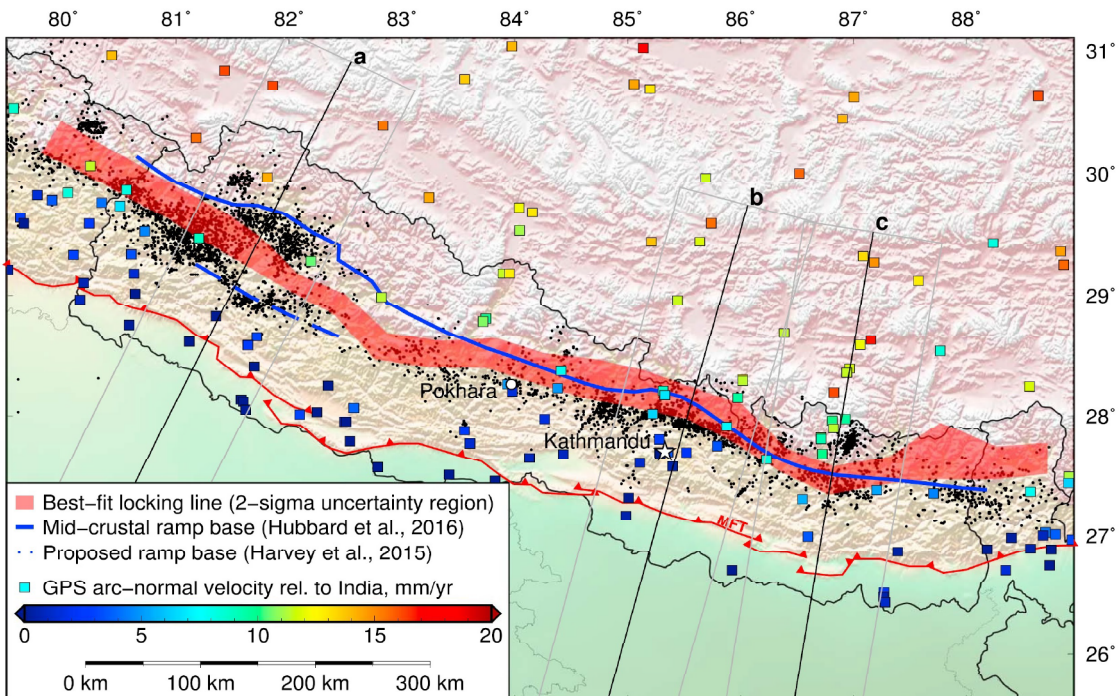


Fig. 2.10: The down-dip extent of the interseismic coupling along the MHT in the central Himalaya (shown in red line). The blue line indicates the down-dip edge of the MHT. The colored rectangles represent GPS velocity vectors and the black dots show observed seismicity during 1996-2008 (Lindsey et al. (2018) [154]).

Feng et al. (2016) [78] analyzed coseismic interferograms and data from GPS stations to characterize the 2015 Gorkha earthquake. They investigated a maximum of ~6 m slip at ~11 km depth rupturing about 150 km eastward from the epicenter [78].

Jouanne et al. (2017) [123] examined about 15 years of GPS data along the Nepal Himalaya and proposed that the MHT is fully locked along the upper part of the flat, partially locked along the mid-crustal ramp, and it is creeping along the lower edge of flat. They have found that the 2015 Gorkha earthquake occurred along the highly coupled upper flat of the MHT, whereas its postseismic rupture propagated towards the eastern side in the lower coupled zone of the MHT [123].

Lindsey et al. (2018) [154] estimated that the fault coupling width varies between 70 to 90 km in the eastern Nepal, 100–110 km in the central Nepal, and narrows down again in the western Nepal (Fig. 2.10). The current findings along the western Nepal suggest that either the shallow portion of the décollement contains an anomalous coupling transition zone or it is partially locked (Fig. 2.10). This phenomenon may be related to the formation of a new sliver along the mid-crustal duplex of the MHT [154]. They inferred 15.2 ± 1.2 mm/yr of reverse faulting with -2.2 ± 2.5 mm/yr of strike-slip motion along the MHT at a depth of 20 km (Fig. 2.10) [154].

Ansari et al. (2018) [11] modeled about 15 years of GPS data with Autoregressive Moving Average (ARMA) method and found that the modeled (with ARMA model) and the observed velocities (with GAMIT/GLOBK post-processing software) agree within ~ 2 mm/yr of uncertainties. They calculated 19 mm/yr slip rate of MHT at 20 km depth and 9.5° dip angle using a 2D dislocation model [11].

Sreejith et al. (2018) [272] determined that the mainshock and aftershocks of the 2015 Gorkha event have partially released the accumulated strain energy in the north of the epicenter. They suggested the possibility of occurrence of similar earthquakes in the west or south where the MHT is fully locked [272].

From the above geodetic studies, it is observed that the slip rate and the locking width of the MHT vary between ~ 13.4 mm/yr to ~ 21 mm/yr and ~ 70 km to ~ 150 km along the central Himalaya. A magnitude 8.0 earthquake along the central Himalaya with a return cycle of ~ 300 years is also suggested by these studies.

2.5 Seismic hazard along the northeast Himalaya

Northeast Himalaya is a seismically active zone because the locking zone of the MHT is more extensive than the other parts along the Himalaya [22, 152]. Due to deeper locking depth of the MHT, this region undergoes strong strain accumulation than other segments

of the Himalaya. The long quiescence of large earthquake along Bhutan and Sikkim in the northeast Himalaya possesses more threat to these regions [25, 30, 33, 129].

2.5.1 Geological studies along the northeast Himalaya

The geological studies along the northeast Himalaya are discussed below from west to east based on their trenching locations (Fig. 2.11).

Based on the findings of some previous studies and new paleoseismic results of a ~ 10 m uplifted scarp in West Bengal along the MFT, ¹Mishra et al. (2016) [172] performed a Bayesian analysis to estimate the rupture length (~ 800 km) and the return period (650 to 2000 years) of the 1255 giant earthquake (Fig. 2.11). Out of this return period, ~ 760 years have been elapsed [172].

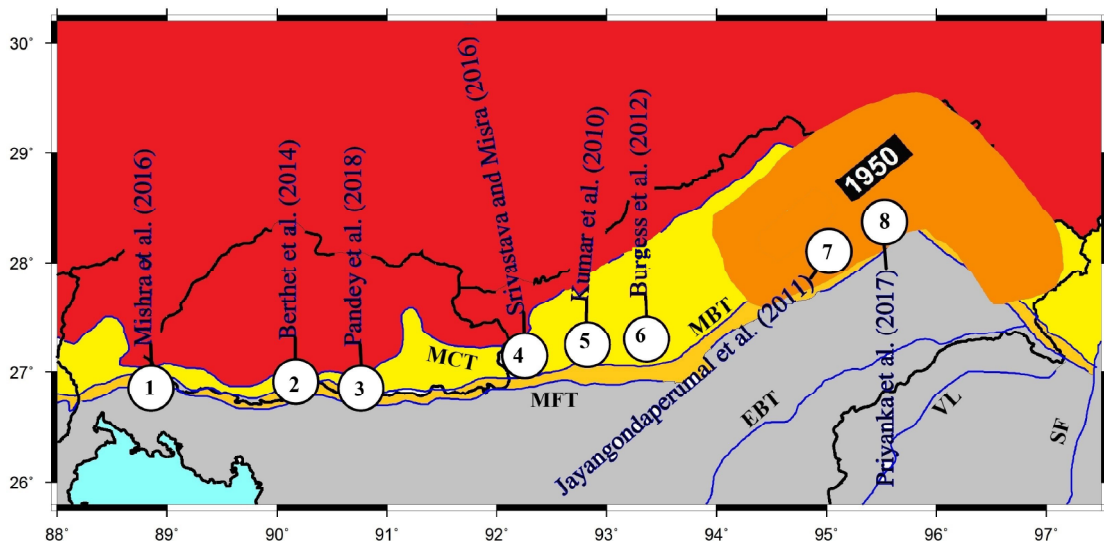


Fig. 2.11: Geological studies along the northeast Himalaya. Abbreviations are as follows: EBT, Eastern Boundary Thrust; MBT, Main Boundary Thrust; MCT, Main Central Thrust; MFT, Main Frontal Thrust; SF, Sagaing Fault; VL, Volcanic Line.

²Berthet et al. (2014) [25] analyzed offsets from fluvial terraces in the south-central Bhutan and showed that two large earthquakes have ruptured MFT during the last millennium (Fig. 2.11). Occurrences of such great Himalayan earthquakes in the past provide 20.8 ± 8.8 mm/yr slip rate of the $25^\circ \pm 5^\circ$ dipping MFT. This slip rate indicates that sufficient seismic energy is accumulated in the region to produce another great event in the near future [25].

³Pandey et al. (2018) [206] collected paleoseismal samples from the Manas and Dhanshiri rivers along the MFT, the area between the 1934 Nepal-Bihar earthquake and the 1950 Assam earthquake (Fig. 2.11). They found that majority of deformation in this region is caused by the north dipping thrust system along with some discontinuous back facing scarps [206]. The long quiescence of large earthquakes and fully compressive tectonics mark this region as a seismic gap, known as the Assam seismic gap. Higher chances of great earthquakes are undeniable in this region [206].

From the study of geomorphic configuration of four alluvial terraces of the Kameng river along the MFT, ⁴Srivastava and Misra (2008) [274] calculated ~ 7.5 mm/yr of uplift rate of Siwalik range in the northeast Himalaya (Fig. 2.11).

⁵Kumar et al. (2010) [140] analyzed two uplifted scarps of 12 m and 14 m along the MFT in the northeastern Himalaya, and observed that these scarps are possibly the same rupture reported earlier [146, 307, 306] from a great event around 1100 AD in Nepal Himalaya (Fig. 2.11).

⁶Burgess et al. (2012) [44] computed long-term slip rate of 23.0 ± 6.2 mm/yr of the MFT using age and geometry of uplifted river terraces in the eastern Himalaya (Fig. 2.11).

⁷Jayangondaperumal et al. (2011) [118] investigated paleoseismic trench of an 8 m uplifted scarp along 30° dipping MFT in the meizoseismal area of the 1950 Assam earthquake and reported that the scarps also have evidence of uplift and folded structure during past historical events post 2009 cal. yr B.P. (calculated year before present) (Fig. 2.11).

⁸Priyanka et al. (2017) [224] utilized radiocarbon dating on a ~ 3.1 m uplifted fault scarp along the Himalayan front at Pasighat and obtained that the 1950 Assam event has propagated through the MFT and produced a 5.5 ± 0.7 m of co-seismic slip that reduces chances of great hazard in this region (Fig. 2.11).

The above geological studies indicate that many blind great earthquakes with large rupture areas have occurred in previous ~ 2000 years along the northeast Himalaya. These studies suggest that the long-term slip rate of 20.8–23.0 mm/yr of the MFT is sufficient to produce a giant earthquake along the Assam seismic gap in the near future.

2.5.2 Geodetic studies along the northeast Himalaya

Jade et al. (2007) [113] estimated 16.0 ± 0.5 mm/yr of convergence rate along the northeast Himalaya and 10–12 mm/yr along the Sikkim region. This convergence rate along

the northeast Himalaya is distributed between the Lesser Himalaya (~ 6 mm/yr) and the Higher Himalaya (~ 10 mm/yr) [113].

Mullick et al. (2009) [189] measured crustal strain in the northeast Himalaya using eight GPS stations. They reported 11.1 ± 1.5 mm/yr of shortening rate (equivalent to the compressional strain of -0.25 ± 0.12 μ strain/yr with the azimuth of 21°) in the western side and 10.9 ± 1.6 mm/yr of lengthening rate (comparable to the extensional strain of 0.36 ± 0.08 μ strain/yr with the azimuth of 103°) in the eastern side of the study region [189].

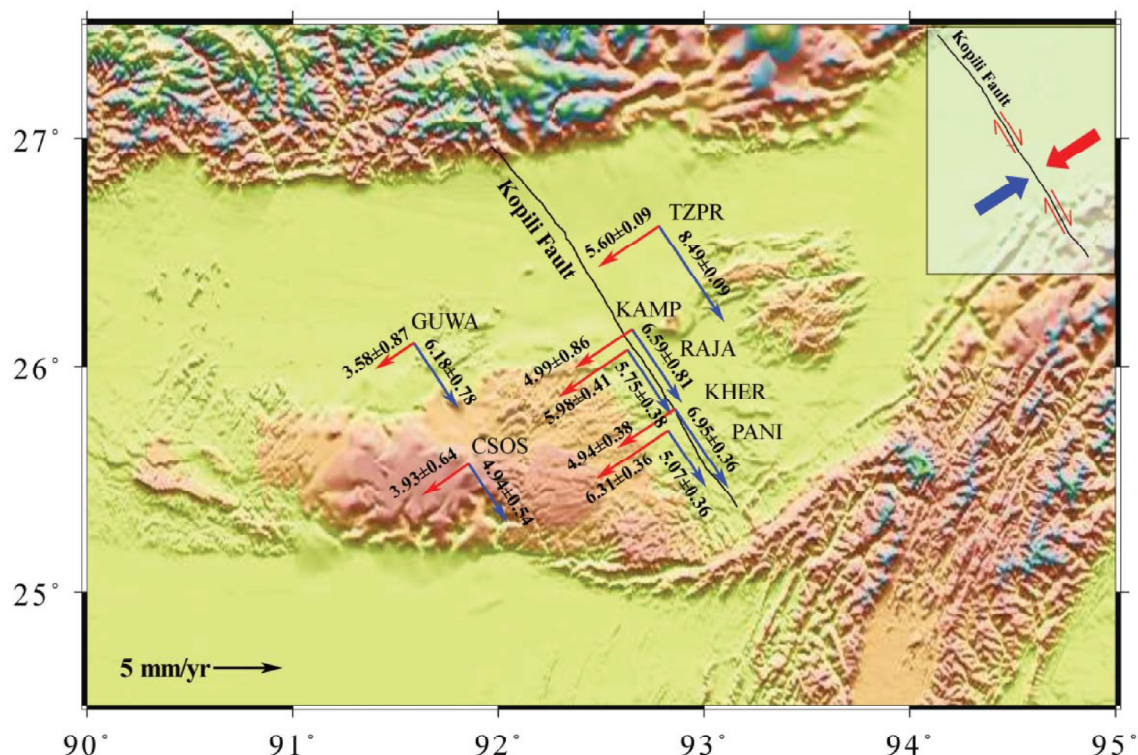


Fig. 2.12: Surface velocity vector representation in fault-normal and fault-parallel components along the strike of the Kopili fault (Barman et al. (2016) [22]).

Mukul et al. (2010) [187] estimated 15–20 mm/yr of convergence rate across the northeast Himalaya from which about 10–20% of shortening is being stored within the Shillong Plateau, whereas ~ 8 – 9 mm/yr convergence is being accommodated in the eastern and the central part of the region.

Gupta et al. (2015) [95] suggested large compression rates (~ 50 – 100 nstrain/yr) along the MFT in the northeast Himalaya. These rates vary from a local maximum of ~ 160 nstrain /yr in the west to ~ 80 nstrain /yr in the east. The dip-slip rate of 32.4 mm/yr

normal to the locked frontal part of the eastern Himalayan sector indicates a recurrence interval of \sim 200 years of the 1950 Assam earthquake [95].

Barman et al. (2016) [22] observed transpressional behavior of the Kopili fault using 12 GPS stations and an elastic dislocation model (Fig. 2.12). They observed that the Kopili fault receives \sim 2.0 mm/yr of dip-slip motion and \sim 2.62 \pm 0.79 mm/yr of right-lateral motion with a 3 \pm 2 km of locking depth (Fig. 2.12). The fault accumulates about \sim 70.74 \times 10¹⁵ Nm/yr of geodetic moment, sufficient to produce $M_w \geq$ 5.17 size earthquake [22]. Further, Barman et al. (2017) [21] re-calculated the dextral motion along the Kopili fault as 4.7 \pm 1.3 mm/yr at a locking depth of 10.2 \pm 1.4 km (Fig. 2.12). They reported that the Shillong Plateau and its surrounding regions act as a rigid block with a \sim 7 mm/yr of southward motion with respect to the fixed Indian plate [21]. Using a dislocation model, they estimated 16 mm/yr of slip rate of the MHT beneath the northeast Himalaya at a 17 km depth and 130 km of locking width [21]. Their estimated \sim 9 mm/yr of convergence rate along the Lesser Himalaya suggests that high strain is accumulated below the MCT [21].

Marechal et al. (2016) [165] identified a non-uniform coupling segment of 100–120 km width in the western Bhutan and a bit wider coupling segment of 135–155 km in the central and eastern Bhutan along the MFT. The complete locking behavior on the MFT and a partial creeping on MBT in the eastern Bhutan suggest that the 2015 Gorkha like event could not reach up to the surface in this region [165].

Panda et al. (2018) [205] proposed that an active sliver has developed along the MFT in the northeast Himalaya which causes the deficiency in the plate convergence between India and Eurasia. They argued that the unusual formation of active sliver along the northeast Himalaya is caused by the strong eastward extrusion of the Tibetan Plateau [205].

Mukul et al. (2018) [186] computed that 6° dipping MHT is creeping with slip rate of \sim 18 mm/yr at \sim 16 km locking depth along the Darjeeling-Sikkim Himalaya. They suggested that this creeping of MHT can cause only minor to moderate earthquakes in this region [186].

Li et al. (2020) [151] utilized GPS observations along the northeast Himalaya (Sikkim, Bhutan, and part of the southern Tibet) to characterize strain accumulation along the MHT. The estimated \sim 100 km locking width of the MHT in the eastern Bhutan is \sim 30–40% wider than that of the western Bhutan and the Sikkim Himalaya. They suggested that part of seismic activity along the Bhutan Himalaya is controlled by the strain

accumulation at the locked part of the MHT [151].

Above geodetic studies indicate that the slip rate and the locking width of the MHT vary from ~ 16 mm/yr to ~ 18 mm/yr and ~ 100 km to ~ 155 km, respectively along the northeast Himalaya. These studies also suggest that out-of-sequence faults (Kopili fault and Oldham fault) largely contributed to holding great Himalayan earthquakes in the past (e.g., the 1897 Shillong Plateau earthquake), and may also contribute to generating future ones.

2.6 Comparison of geologic and geodetic rates along the Himalayan arc

Comparison of long-term geological rates and short-term geodetic rates proposes a means of determining whether the GPS rates provide a satisfactory validation of tectonic movements and kinematics of deformation over a long Holocene timescale [155, 303]. However, this comparison has produced conflicting findings, which may be similar or different, indicating that the tectonic plates may have deformed differently on different time periods [155, 197]. The common hypothesis for this difference is that the geological rates reflect only long-term permanent deformation on the crust, whereas the GPS-derived rates include both permanent as well as elastic crustal deformation. The elastic deformation eventually gets converted to permanent deformation during future earthquakes [155, 197]. Most of the geological studies along the Himalayan arc have been carried out along the frontal part as trenching in a mountain region is often a tedious task. A segment-wise comparison of geological and geodetic slip is provided in Table 2.1 to Table 2.3.

A comparison of geological and geodetic slip rates along the northwest, central, and the northeast Himalaya is provided below.

1. In the Kashmir Himalaya, the observed slip rate of the MHT from the geological studies [296, 297] is about $\sim 30\%$ higher than that of the geodetic studies [20, 143, 254], whereas the long-term slip rate of the MFT is much higher ($\geq 50\%$) than the short-term slip rate. In the nearby segment, Himachal Himalaya, geological studies are available, however, no GPS stations (except the present network) are installed in this region to provide a comparison. Geologically observed slip rate of the MFT is much higher in the Garhwal-Kumaun Himalaya, providing ~ 11 mm/yr of slip deficit rate.

2. Along the central Himalaya, most of the geodetic studies [2, 11, 26, 32, 35, 50, 62, 91, 124, 144, 152, 154, 277] have utilized single fault model (explained in Chapter 3) in which the MFT is considered to be fully locked (i.e., no fault slip). These studies generally compare the long-term geological slip rate of the MFT with the geodetic slip rate of the MHT. Along the western Nepal and the central Nepal, the geological slip rate of the MFT and the geodetic slip rate of the MHT are comparable, whereas along the eastern Nepal, geological slip rate of the MFT is about 75% lesser than the geodetic slip rate of the MHT.
3. Similar to central Himalaya, the MFT is also considered to be locked along the northeast Himalaya [62, 113, 152, 154, 186, 187, 277]. The long-term slip rate of the MFT is consistent with the short-term slip rate of the MHT along the northeast Himalaya.

Overall, the long-term geological slip rates of the MFT and short-term geodetic slip rates of the MHT are comparable along the western Nepal, central Nepal, and the northeast Himalaya. However, along the northwest Himalaya and the eastern Nepal, geological slip rates of the MFT are 35% and 75% lesser than the corresponding geodetic slip rates of the MHT.

Table 2.1: Comparison of geological and geodetic rates along the northwest Himalaya

Section	Geological Slip rates (mm/yr)	Geodetic Slip rates (mm/yr)
Kashmir Himalaya	MHT = 20.2 ± 7.0 [296] MFT = 9.0 ± 3.2 [296] MWT = 11.2 ± 3.8 [296]	$\text{MHT} = \begin{cases} 14.0 \pm 1.0 & [20]; \\ 15.7 \pm 1.0 & [254]; \\ 17.0 \pm 2.0 & [143] \end{cases}$ $\text{MFT} = 4.0 \pm 2.0$ [254]
Himachal Himalaya	$\text{MFT} = \begin{cases} 14.0 \pm 2.0 & [223]; \\ 7.0 \pm 1.7 & [162]; \\ 6.9 & [283]; \\ 12.6 \pm 6.0 & [141]; \\ 9.6 \pm 3.5 & [142] \end{cases}$ $\text{JMT} = 4.2$ [283]	—
Garhwal- Kumaun Himalaya	$\text{MFT} = \begin{cases} 13.8 \pm 3.5 & [310]; \\ 11.0 \pm 5.0 & [223]; \\ 12.5 \pm 2.6 & [210] \end{cases}$	$\text{MHT} = \begin{cases} 16.0 - 18.0 & [114]; \\ 18.0 & [88, 316]; \\ 15.4 \pm 2.3 & [69]; \\ 18.5 \pm 1.8 & [277]; \\ 17.2 \pm 1.0 & [219]; \\ 21.8 - 22.6 & [154]; \\ 13.1 \pm 0.8 & [62] \end{cases}$ $\text{MFT} = 1.5 \pm 1.0$ [69] $\text{MBT} = 5.2 \pm 1.2$ [69] $\text{MCT} = 8.7 \pm 1.7$ [69]

Table 2.2: Comparison of geological and geodetic rates along the central Himalaya

Section	Geological Slip rates (mm/yr)	Geodetic Slip rates (mm/yr)
Western Nepal	MFT=19.0±6.0 [180]	MHT = $\begin{cases} 20.5 \pm 2.0 [35, 32]; \\ 23.0 \pm 2.0 [144]; \\ 12.4 \pm 0.4 [50]; \\ 19.0 [11, 124]; \\ 13.4 \pm 5.0 [26]; \\ 20.5 \pm 1.0 [2]; \\ 20.2 \pm 1.1 [277]; \\ 19.8 \pm 0.8 [154]; \\ 19.0 \pm 1.5 [11, 62] \end{cases}$
Central Nepal	MFT=21.0±1.5 [145]	MHT = $\begin{cases} 21 \pm 3 [35]; \\ 12.4 \pm 0.4 [50]; \\ 19.3 [26]; \\ 17.8 \pm 0.5 [2]; \\ 19.5 \pm 1.5 [91, 124]; \\ 19.4 \pm 1.4 [277]; \\ 20.2 [152]; \\ 17.7 [154]; \\ 18.2 \pm 6.0 [62] \end{cases}$
Eastern Nepal	MFT=5.0 [191]	MHT = $\begin{cases} 21.0 \pm 3.0 [35, 144]; \\ 19.0 \pm 2.5 [26]; \\ 17.8 \pm 0.5 [2]; \\ 17.6 \pm 0.9 [277]; \\ 22.2 \pm 1.7 [152]; \\ 16.9 \pm 0.4 [154]; \\ 18.2 \pm 6.0 [62] \end{cases}$

Table 2.3: Comparison of geological and geodetic rates along the northeast Himalaya

Section	Geological Slip rates (mm/yr)	Geodetic Slip rates (mm/yr)
Northeast Himalaya	$MHT = \begin{cases} 23.0 \pm 6.2 [44]; \\ 20.8 \pm 8.8 [25] \end{cases}$	$MHT = \begin{cases} 16.0 \pm 0.5 [113]; \\ 17.5 \pm 2.5 [187]; \\ 21.2 \pm 2.0 [277]; \\ 22.2 \pm 1.7 [152]; \\ 18.0 [186]; \\ 17.6 \pm 0.2 [154]; \\ 20.8 \pm 8.9 [62] \end{cases}$

2.7 Summary

This chapter has provided a thorough literature review of seismic hazard studies along the Himalayan arc. First, some important geological and geodetic studies related to seismic hazard are discussed along the whole Himalayan arc. Further, discussion of seismic hazard from geological and geodetic investigations is carried out along the three subsections (i.e., the northwest Himalaya, central Himalaya, and the northeast Himalaya) of the Himalayan arc. A brief summary of the literature review is provided below.

(i) Along the northwest Himalaya, the long-term geological and short-term geodetic slip rates of the MFT reveal that it has accumulated a large slip deficit. This slip deficit is sufficient to produce a great earthquake in the near future with a return period of 500–700 years along the northwest Himalaya. In addition, the fault slip along the décollement is observed to vary between ~ 11 mm/yr to ~ 18 mm/yr with 110–170 km of locking width along the northwest Himalaya.

(ii) Along the central Himalaya, there have been evidences of many blind great earthquakes since ~ 1100 years with recurrence intervals lying in ~ 300 –900 years. The large slip deficit rate along the MFT suggests the possibility of a great event in the near future in this region. Further, the fault coupling and the slip rate of the MHT along the central Himalaya vary between ~ 70 km to ~ 150 km and ~ 13.4 mm/yr to ~ 21.0 mm/yr, respectively.

(iii) Along the northeast Himalaya, evidences of past blind great earthquakes are reported. The long-term strain accumulation and large slip deficit rate along the MFT suggest the possibility of great earthquakes along this region. With a slip rate of 16–18 mm/yr, the MHT is fully locked up to 100–155 km from the surface trace of the MFT to further north along the northeast Himalaya.

This chapter has provided brief discussion on available geological and geodetic studies related to seismic hazard analysis along different sections of the Himalayan arc. The next chapter, Chapter 3, will discuss the regional GPS network, data collection and processing along with the associated crustal deformation results in terms of surface velocity map and strain rate distribution.